Biosystems Engineering (2006) **93** (2), 161–171
doi:10.1016/j.biosystemseng.2005.11.004
PH—Postharvest Technology

Hyperspectral Scattering for assessing Peach Fruit Firmness

Renfu Lu[1]; Yankun Peng[2]

[1]USDA/ARS, 224 Farrall Hall, Michigan State University, East Lansing, MI 48824, USA; e-mail of corresponding author: lur@msu.edu
[2]Department of Biosystems and Agricultural Engineering, Michigan State University, East Lansing; e-mail: MI 48824, USA; e-mail: pengy@egr.msu.edu

(Received 29 March 2005; accepted in revised form 3 November 2005; published online 4 January 2006)

Light scattering is related to the structural characteristics of fruit and hence is potentially useful for estimating fruit firmness. This research investigated hyperspectral scattering as a means for measuring peach fruit firmness. A hyperspectral imaging system was used to simultaneously acquire 153 spectral scattering profiles, generated by a broadband light beam, from 'Red Haven' and 'Coral Star' peaches between 500 and 1000 nm. The spectral scattering profiles at individual wavelengths were fitted accurately by a two-parameter Lorentzian distribution function with the average value for the coefficient of determination r^2 greater than 0·990. Firmness prediction models were developed, using multi-linear regression coupled with cross validation, on relating individual Lorentzian parameters and their combinations at different wavelengths to peach fruit firmness. The wavelength of 677 nm, corresponding to chlorophyll absorption, had the highest correlation with fruit firmness among all single wavelengths. However, a combination of 10 or 11 wavelengths was needed in order to obtain best predictions of fruit firmness. Best firmness predictions were obtained with values for r^2 of 0·77 and 0·58 for 'Red Haven' and 'Coral Star' peaches when Lorentzian parameters a and b were used as independent variables where a and b are the peak scattering value and the full width of the scattering profile at one half of the peak value, respectively. Hyperspectral scattering is potentially useful for rapid, non-destructive estimation of peach fruit firmness.

1. Introduction

Firmness is an important textural attribute for peach fruit and directly influences their shelf life and consumer acceptance. Currently, peach firmness is routinely determined by the destructive Magness–Taylor (MT) firmness tester, which records maximum force for a steel probe of specific size and shape to penetrate fruit, for a pre-determined distance. Although the MT firmness tester is prone to operational error and does not have good repeatability, it is still the most widely used technique for measuring fruit firmness.

Non-destructive sensing of fruit firmness would provide the fruit industry with a means to ensure the quality and consistency of individual fruit, increase consumer satisfaction, and thus improve industry profitability. Considerable research has been reported on developing non-destructive sensing techniques for measuring fruit firmness. The majority of reported studies have been focused on using mechanical methods including quasi-static force/deformation, impact, and sonic test (Abbott *et al.*, 1997; Lu & Abbott, 2004). As the MT tester and non-destructive mechanical methods measure different mechanical properties, their correlation varies widely with values for the coefficient of determination r^2 in the range between 0·30 and 0·85 for a variety of fruits (Hung *et al.*, 2001; Shmulevich *et al.*, 2003).

Over the past 15 years, near-infrared (NIR) spectroscopy has received increased attention as a means for measuring internal quality of fresh fruit, especially flavour-related quality attributes such as soluble solids content (Dull *et al.*, 1989; Kawano *et al.*, 1992; Lammertyn *et al.*, 1998; Lu, 2001; Lu *et al.*, 2000; Moons *et al.*, 1997; Slaughter, 1995). Research on using NIR spectroscopy to measure fruit firmness has also

been reported, but the results are still not satisfactory (Lu & Ariana, 2002; Lu *et al.*, 2000; McGlone & Kawano, 1998).

When a light beam impinges on the fruit, a small fraction will be reflected at the surface (specular reflectance) and the majority of the light will penetrate into the fruit. The penetrated light will scatter and propagate in different directions in the fruit owing to the change in the index of refraction at the interfaces of different cellular structures. Some of the penetrated light will be absorbed, some will go through the whole fruit and emerge from the opposite side (transmission), and some will scatter back and reemerge from the region close to the beam incident point, which is often called diffuse reflectance. Multiple scattering takes place in dense scattering media such as fruit. The fruit-softening process is accompanied with the change in the tissue density and the weakening of cells and other cellular structures, which in turn would affect light scattering. Soft fruit tend to have a broader scattering profile than firmer fruit (Peng & Lu, 2004). However, the interaction of light with the fruit tissue is complicated by the fact that photons are also being absorbed during the multiple scattering process. The spatial intensity profile of diffuse reflectance (or simply the scattering profile) at the surface of the fruit is influenced by, or related to, both absorption and scattering properties of the fruit. Quantification of light scattering and absorption in the fruit may be achieved by measuring spatially resolved diffuse reflectance (Tuchin, 2000). Such quantification could lead to improved assessment of fruit firmness.

Several researchers investigated the potential of using light scattering to measure fruit firmness and/or maturity. A laser diode was used as the light source, and monochromatic scattering at the surface of the fruit was acquired by using either a colour charge-coupled device (CCD) camera (Cho & Han, 1999; Tu *et al.*, 1995) or a single channel CCD detector (McGlone *et al.*, 1997). These studies showed that light scattering is related to fruit firmness, but the correlation is still low or inconsistent. Other researchers (Cubeddu *et al.*, 2001; Valero *et al.*, 2004) used time-resolved laser reflectance spectroscopy to measure the optical properties (absorption and scattering coefficients) of fruit and then relate them to internal quality of the fruit. While the time-resolved reflectance spectroscopy technique is promising, the instrumentation is still expensive and difficult to use, and it is time consuming to collect optical properties (Cubeddu *et al.*, 2001).

Lu (2004) proposed a new concept of using multi-spectral imaging to measure scattering from apple fruit at five selected wavelengths in the visible/NIR region. Spectral scattering images were reduced to one-dimensional scattering profiles. By using the artificial neural network method, scattering profiles were related to fruit firmness of apples; good firmness predictions were obtained with a value for r^2 of 0·76 for Red Delicious apples. Peng and Lu (2005) further compared three mathematical models for describing scattering profiles from apple fruit. They reported that a three-parameter Lorentzian distribution function was best in describing multi-spectral scattering profiles and for estimating fruit firmness.

While multi-spectral imaging enables us to acquire spectral images at a few (normally less than ten) selected, discrete wavelengths, hyperspectral imaging has become a powerful tool for acquiring both spectral and spatial information from an object at contiguous wavelengths over a wide spectral range. The technique is thus useful for quantifying or detecting spatial variations of properties in food and agricultural products, and it has been researched extensively for quality evaluation and safety inspection of agricultural and food products (Lawrence *et al.*, 2003; Lu, 2003; Lu & Chen, 1998; Martinsen & Schaare, 1998; Peirs *et al.*, 2003).

This paper reports the results from a study of using hyperspectral scattering for estimating peach fruit firmness. Compared to few selected wavelengths used in multi-spectral scattering (Lu, 2004), the hyperspectral imaging technique used in this research simultaneously acquired scattering profiles for all 153 wavebands in 500–1000 nm at a spectral resolution of 3·28 nm. Owing to the large amount of information acquired by the hyperspectral imaging system, the technique is particularly useful in identifying key wavelengths for firmness prediction. Specific objectives of this research were to:

(a) acquire hyperspectral scattering images from peach fruit over the visible and short-wave NIR region between 500 and 1000 nm;
(b) propose an empirical mathematical model to describe scattering profiles from peach fruit at individual wavelengths; and
(c) develop firmness prediction models relating parameter spectra of hyperspectral scattering profiles to peach fruit firmness.

2. Materials and methods

2.1. *Peach samples*

The experiment was carried out during the 2003 and 2004 harvest seasons. In 2003, 'Red Haven' peaches were hand-harvested three times over 1 week period from the orchard of Michigan State University Teaching and Research Farm in East Lansing, Michigan. Peach

samples were visually inspected, and only those of regular shape and free of visual defects were selected for the experiment. In 2004, a different cultivar, 'Coral Star', was used because the cultivar used in the previous year was not available for the research. The same harvest procedure was used in 2004. A total of 450 'Red Haven' peaches were used in 2003, and 440 'Coral Star' peaches in 2004.

2.2. *Hyperspectral imaging system*

A hyperspectral imaging system developed in the US Department of Agriculture/Agricultural Research Service (USDA/ARS) postharvest engineering laboratory at Michigan State University, East Lansing, Michigan was used for this study (*Fig. 1*). The system mainly consisted of a high-performance back-illuminated CCD camera and its control unit (model C4880-21, Hamamatsu Corp, Japan), an imaging spectrograph (ImSpector V9, Spectral Imaging Ltd., Finland), a specially assembled light unit with a quartz tungsten halogen lamp as the light source (Oriel Instruments, USA), and the sample holder (*Fig. 1*). The imaging spectrograph acquired spectral information by line-scanning the fruit and dispersing the light from the scanned line into different wavelengths, using a prism–grating–prism configuration while preserving its original spatial information. The dispersed light signals were then projected onto the CCD detector, creating a special two-dimensional image; one dimension represents the spatial and the other spectral [*Fig. 2*(*a*)]. The light source used in this study was a circular beam of 1·6 mm diameter with the divergence angle less than 17°. As the beam hit the fruit, it illuminated a portion of the fruit surrounding the incident point as a result of light scattering and propagation in the fruit tissue. This generated a backscattering image at the surface of the fruit. With the camera-exposure time and amplification gain being properly adjusted, the hyperspectral imaging system line-scanned the fruit 1·5 mm off the incident centre so that the CCD detector pixels would not be saturated by high-intensity signals in the beam centre (*Fig. 1*). The effective spectral region covered by the hyperspectral imaging system was between 500 and 1000 nm.

The hyperspectral imaging system was calibrated both spectrally and spatially by following the procedures described in Lu and Chen (1998). Spectral calibrations were performed using spectral lamps (xenon, argon, krypton, and mercury), a fluorescent lamp, and a laser diode at 905 nm. For the spatial calibration, a white paper printed with thin parallel lines of 2 mm apart was placed at the sample holder. The calibration results showed that the system was highly linear and the distortion of spectral and spatial information was within one pixel on the CCD detector. Thus, no spectral and spatial corrections were needed for the system. The hyperspectral imaging system had a spectral resolution of 1·64 nm per pixel and a spatial resolution of 0·13 mm per pixel.

2.3. *Experimental procedure*

The peaches used in the experiment had surface hair or trichomes, which may lead to increased noise in the image and, to a lesser degree, affect the scattering profile

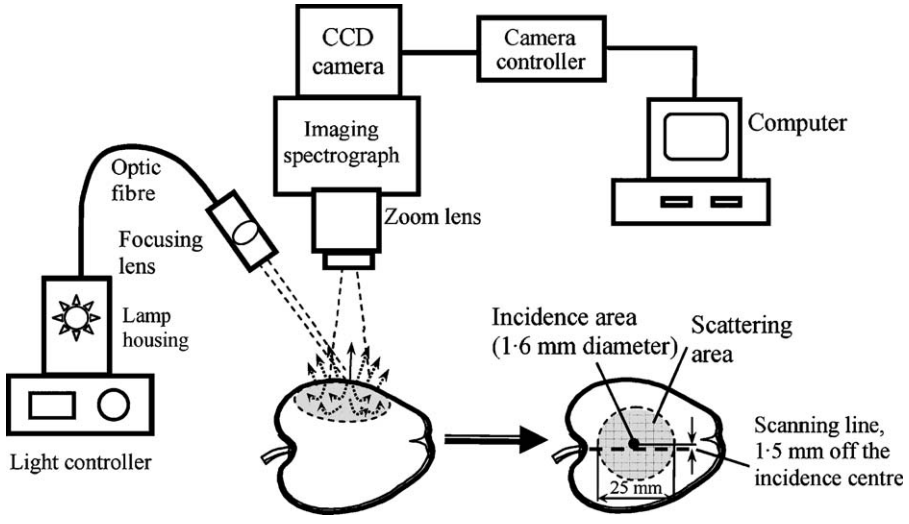

Fig. 1. Schematic of the hyperspectral imaging system for acquiring scattering images from peach fruit; CCD, charge coupled device

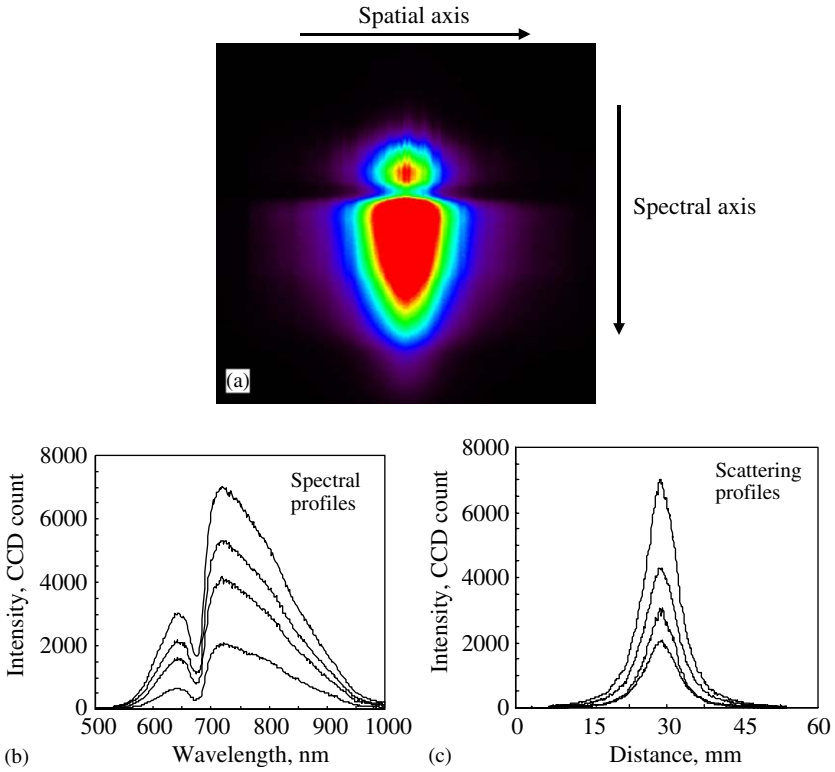

Fig. 2. Hyperspectral scattering image of a peach fruit (a), where the vertical axis represents spectral and the horizontal axis spatial; raw (unsmoothed) spectral profiles from different spatial locations are shown in (b) and raw spatial scattering profiles at four wavelengths are shown in (c); intensities are expressed as CCD count, with no unit

when they are imaged. Hence, the peaches were first cleaned by a cloth to remove surface hair. This experimental procedure is compatible with what is practiced in modern packinghouses where fruit are washed and brushed to remove surface dirt or hairy tissue before being inspected by a machine vision system. After the peaches were cleaned, an equatorial location free of visible defect and irregular surface characteristics was selected on each fruit for imaging and the subsequent MT testing, without regarding skin colour. Each fruit was placed on the holder with the stem-calyx end horizontal. The holder had an opening of 30 mm diameter. Each fruit was imaged four times and these images were then averaged. Only average images were saved for further analysis.

After hyperspectral images had been taken, MT firmness measurements were performed on the peaches from the same imaging area by using an 11 mm steel probe mounted onto a tabletop universal testing machine. A small part of the fruit peel was removed before the MT measurement was performed on each fruit. The probe was penetrated into the fruit for a depth of 8·0 mm at a loading rate of 2·0 mm/s, and maximum forces recorded were used as a reference measure of fruit firmness.

2.4. *Mathematical model for scattering profiles*

To improve the signal-to-noise ratio, the original 512×512 scattering images were first reduced to 256×256 images by the 2×2 pixel averaging [*Fig. 2(a)*]. A region of interest (ROI) was then selected from each image, covering a spectral region of 500–1000 nm and the total spatial dimension of 30 mm. Each ROI contains a large amount of information about the fruit. A vertical line taken from the image represents a spectral profile for a particular point of the scanning line from the surface of the fruit. In essence, each scattering image is composed of hundreds of spectra; each spectrum comes from a different position at the fruit surface [*Fig. 2(b)*]. On the other hand, a horizontal line from the image represents the spatial scattering profile for a specific wavelength [*Fig. 2(c)*]. There were 153 scattering profiles from each ROI image covering the spectral range between 500 and 1000 nm at a spectral resolution of 3·28 nm. The following mathematical model, *i.e.* a Lorentzian distribution function, was proposed to fit each scattering profile:

$$I_{w_i} = \frac{a_{w_i}}{1 + (x/b_{w_i})^2} \tag{1}$$

where: I is the light intensity in the CCD count; x is the scattering distance measured from the beam incident centre, in mm; a represents the peak value of the scattering profile at $x = 0$ in the CCD count; b is the full width of the scattering profile at one half of the peak value, in mm; the subscript w_i represents a specific wavelength in the range between 500 and 1000 nm with $i = 1, 2, 3, \ldots, N$ where N is the total number of wavelengths (153). The Lorentzian function is widely used for describing laser beam profiles and light scattering in optics. Peng and Lu (2005) showed that a Lorentzian function with three parameters fitted scattering profiles accurately for selected wavelengths acquired by a multi-spectral imaging system.

Nonlinear regression was performed for fitting the two-parameter Lorentzian function to each scattering profile for individual peaches at each wavelength. Thus, the scattering profile at each wavelength was completely described by two Lorentzian parameters a and b. After completing the curve fitting for all 153 wavelengths, values for the two parameters, a and b, were assembled to form two parameter spectra for each fruit. These spectra were further analysed for predicting peach fruit firmness.

2.5. *Firmness prediction models*

After the two parameter spectra a and b were obtained, statistical methods were used to develop firmness prediction models for each cultivar. Since there are two parameter spectra in comparison to one spectrum from NIR spectroscopy, a different approach was needed on relating these parameter spectra to fruit firmness. First, firmness prediction models were developed utilising each parameter spectrum (a and b). Next, the multiplication of parameters a and b, designated as $a \times b$, was used for developing another firmness prediction model. The parameter multiplication $a \times b$ reduces two spectra to one, which represents the area enclosed by the scattering profile. Finally, parameter spectra a and b were treated as two independent variables, referred to as a & b, which means that there are two values or variables from a and b, respectively, at each wavelength instead of one value as in the previous three prediction models. Firmness predictions from these four models were compared in order to determine the best means of relating parameter spectral data to fruit firmness.

To develop a firmness prediction model, all peach samples for each cultivar (450 in 2003 and 440 in 2004) were first separated into two groups randomly as: 75% for calibration and 25% for validation. The following five steps were then taken to develop the firmness calibration model.

(1) Multi-linear regression (MLR) was applied to the calibration samples to calculate the values for r^2 and the standard error of calibration (SEC) between scattering parameter(s) and MT firmness for each wavelength. The values for r^2 (or SEC) were ranked in descending (or ascending) order for all wavelengths. The wavelength that had the highest value for r^2 (or the lowest for SEC) was selected as the best single wavelength. While the MLR method is not very efficient in multi-variate calibration compared to such methods as principal component regression (PCR) and partial least squares (PLS), it could better suit the needs of this research. First, since there are two parameter spectra, *i.e.* a and b, the use of PCR or PLS could be a problem when dealing with the parameter combination a & b. Second, the MLR method ranks individual wavelengths in the order of their importance for estimating fruit firmness. This information is especially useful for the development of a sensing system that only uses selected wavelengths (Lu, 2004). The MLR equation for the first three prediction models (*i.e.* a, b, and $a \times b$) is given below:

$$F = C_0 + \sum_{j=1}^{J} C_j X_{w_j} \tag{2}$$

and for the fourth model (a & b),

$$F = C_0 + \sum_{j=1}^{J} C_j a_{w_j} + \sum_{j=1}^{J} D_j b_{w_j} \tag{3}$$

where: F is the MT firmness in N; C_0, C_j and D_j are the regression coefficients with $j = 1, 2, 3, \ldots, J$ in which J is equal to the number of optimal wavelengths selected for each model; X represents a or b or $a \times b$; and w_j refers to a selected wavelength. The fourth model in Eqn (3) has $(2 \times J + 1)$ terms compared to $(J+1)$ terms for Eqn (2) when the same number of wavelengths is selected.

(2) A search for the best two wavelengths was started. Individual wavelengths were sequentially added to the best single wavelength, and the corresponding values for r^2 and SEC were calculated for all two-wavelength combinations. The best two wavelengths were determined when they gave the highest values for r^2 and the lowest for SEC among all two-wavelength combinations. This process repeated until the calibration model with all wavelengths was obtained.

(3) Cross-validation was applied to the calibration set, starting from the best single wavelength, to ensure

that no over-fitting would occur to the calibration model. Each time, one sample was taken out from the calibration set. A calibration model was established for the remaining samples and the model was then used to predict the sample left out. Thereafter, the sample was placed back into the calibration set and a second sample was taken out. The procedure was repeated until all samples have been left out once. The root mean square error of cross-validation (SECV) was calculated for each of all wavelength combinations.

(4) The combination of wavelengths that gave the least value for the SECV was selected to be the optimal combination of wavelengths.

(5) A prediction model with the optimal wavelengths was established by the MLR method for all calibration samples, and it was then validated by the validation set.

3. Results and discussion

The MT firmness of the 450 'Red Haven' peach samples ranged from 5·4 to 110·0 N, with the mean of 44·7 N and the standard deviation (SD) of 29·0 N. The MT firmness for 'Coral Star' peaches ranged between 5·0 and 99·7 N, with the mean of 47·2 N and the SD of 28·2 N.

3.1. *Scattering profiles*

Typical curve fitting results from the Lorentzian function for the scattering profiles of a peach fruit at wavelengths of 710 and 850 nm are shown in *Fig. 3*. The Lorentzian function fitted the scattering profiles accurately at both wavelengths. Overall, the two-parameter Lorentzian distribution function fitted the scattering profiles accurately for wavelengths between 600 and 1000 nm (*Fig. 4*). The average value of the correlation coefficient for these peaches was greater than 0·990 for wavelengths greater than 600 nm. For wavelengths below 600 nm, the Lorentzian function did not fit the scattering profiles as well as for wavelengths greater than 600 nm. This is primarily because light signals at these wavelengths were much lower with considerable noise. As a result, only the data between 600 and 1000 nm were used in the development of firmness prediction models. Similar results were also obtained for 'Coral Star' peaches in 2004.

Figure 5 shows the spectra of *a* and *b* for selected 'Red Haven' peach samples. While the parameter *a* had dramatic changes in its value over the spectral region between 600 and 1000 nm, the magnitude of change for

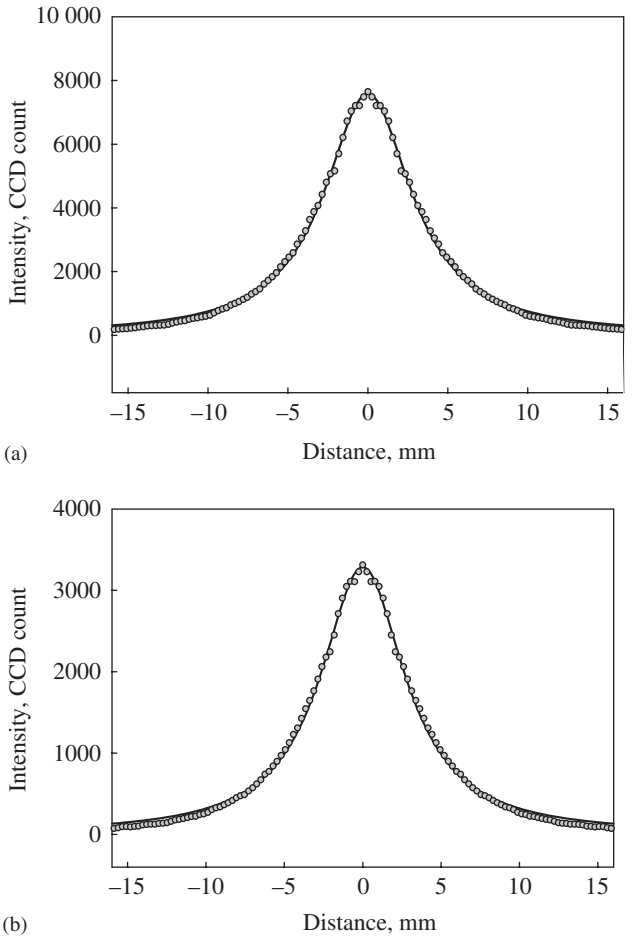

Fig. 3. Curve fitting results from the Lorentzian function at wavelengths of 710 nm (a) and 850 nm (b) for a peach fruit with Magness–Taylor firmness of 84·0 N; intensities are expressed in CCD count, with no unit

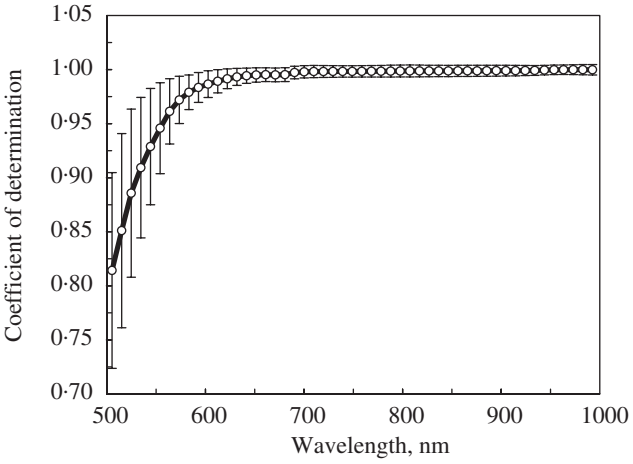

Fig. 4. Coefficients of determination obtained from fitting scattering profiles by the Lorentzian function over the spectral region between 500 and 1000 nm for 450 peaches; Vertical bars in the figure represent two standard deviations for r^2

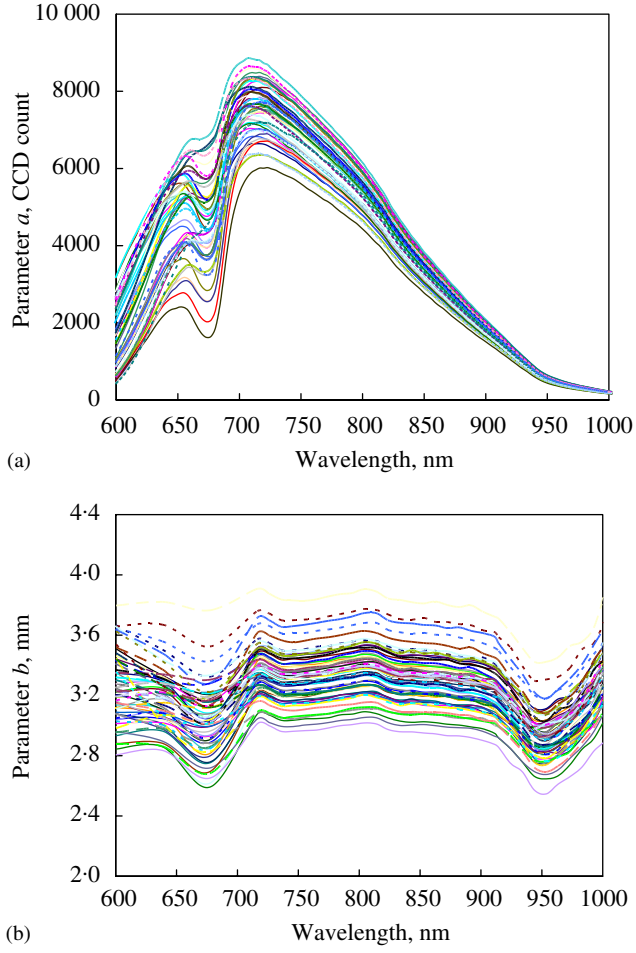

Fig. 5. Spectra of Lorentzian parameters a and b for selected peach samples; a represents the peak scattering intensity in CCD count, with no unit; b is the full width of the scattering profile at one half of the peak intensity, in mm

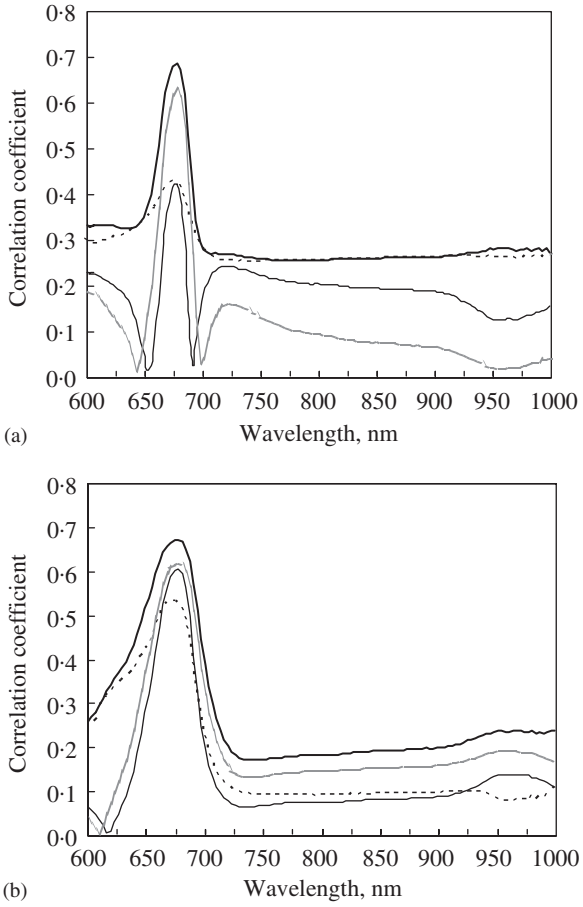

Fig. 6. Simple correlation coefficient spectra obtained for the four parameter combinations over the wavelengths between 600 and 1000 nm for 'Red Haven' (a) and 'Coral Star' (b) peaches; —, a, the peak value of scattering profiles; - - - , b, the full width at one half of the peak value; ——, a × b, the multiplication of a and b; ▬▬, a & b, two independent parameters for each wavelength

the parameter *b* was much smaller. There are two large concave peaks around 677 and 950 nm on the spectra of parameter *b*, which correspond to chlorophyll and water absorption bands, respectively.

3.2. *Estimated fruit firmness versus individual wavelengths*

Figure 6 shows the simple correlation coefficient between four combinations of scattering parameters (*i.e.* *a*, *b*, $a \times b$, and *a* & *b*) and MT firmness over wavelengths 600–1000 nm for 'Red Haven' and 'Coral Star' peaches. For 'Red Haven' peaches, parameter *b* had a consistently higher correlation with MT firmness than that of parameter *a* for the entire wavelength range 600–1000 nm. The pattern of the correlation spectrum for $a \times b$ is interesting; it had lowest values of the correlation coefficient with MT firmness over the entire spectral region, except for the wave band around 677 nm at which the correlation ($r = 0{\cdot}63$) was considerably higher than that for parameters *a* and *b*. The combination *a* & *b* yielded the overall highest value for the correlation coefficient over the entire spectral region between 600 and 1000 nm, even though its difference with parameter *b* was minimal between 740 and 930 nm [*Fig 6(a)*]. At 677 nm, the parameter combination *a* & *b* had the highest correlation to MT firmness, with a value for *r* of 0·69.

The overall pattern of the correlation for the four parameter combinations *versus* wavelength for 'Coral Star' peaches was similar to that for 'Red Haven' peaches [*Fig. 6(b)*]. The combination $a \times b$ correlated with MT firmness consistently better than the other

three combinations. At 677 nm, the four parameter combinations, in the order of the magnitude of correlation coefficient, were a & b, $a \times b$, a, and b. For the wavelengths between 700 and 950 nm, the order of the four parameter combinations was a & b, $a \times b$, b, and a.

The results in *Fig. 6* showed that wavebands around 677 nm had a most significant impact on the MT firmness compared to other wavebands. This observation is not totally surprising since chlorophyll content is related to fruit maturity. The fruit maturing process is accompanied with the decrease in chlorophyll content. As the chlorophyll content decreases, fruit firmness also changes.

3.3. *Firmness predictions with optimal wavelengths*

Results in *Fig. 6* indicate that the best single wavelength was 677 nm for all four parameter combinations. This single wavelength is, however, not sufficient for accurate estimation of MT firmness. The cross validation method was used to find a set of optimal wavelengths that would yield best predictions of peach fruit firmness. When the parameter combination $a \times b$ was used for estimating peach fruit firmness, the best correlation was obtained with 10 wavelengths (603, 616, 629, 642, 648, 664, 671, 677, 690, 707 nm) for 'Red Haven' peaches and 11 wavelengths (625, 645, 661, 671, 674, 677, 947, 957, 976, 980, 996 nm) for 'Coral Star' peaches (*Fig. 7*). The best 10 wavelengths for 'Red Haven' were concentrated in the 100 nm range between 603 and 707 nm. For 'Coral Star', there were six wavelengths between 625 and 677 nm and five between 947 and 996 nm. The best top four wavelengths in the order of importance were 677, 690, 629 and 671 nm for 'Red Haven' and 677, 957, 947 and 980 nm for 'Coral Star'. Similarly, ten wavelengths were needed to obtain improved firmness predictions with the other three parameter combinations. The chlorophyll absorption band occurs around 675 nm whereas there is a water absorption band around 950 nm. The wavelength selection results suggest that for 'Red Haven' peaches, the chlorophyll absorption band had a significant influence on fruit firmness whereas for 'Coral Star', both chlorophyll and water absorption bands had an important effect on firmness. Chlorophyll content and water status in the fruit are related to fruit firmness, but their correlation is not sufficiently high. This is quite clear from the relatively large number of wavelengths selected for firmness predictions.

With these optimal wavelengths, the calibration models were used to predict peaches from the validation set. *Figure 8* shows firmness prediction results obtained

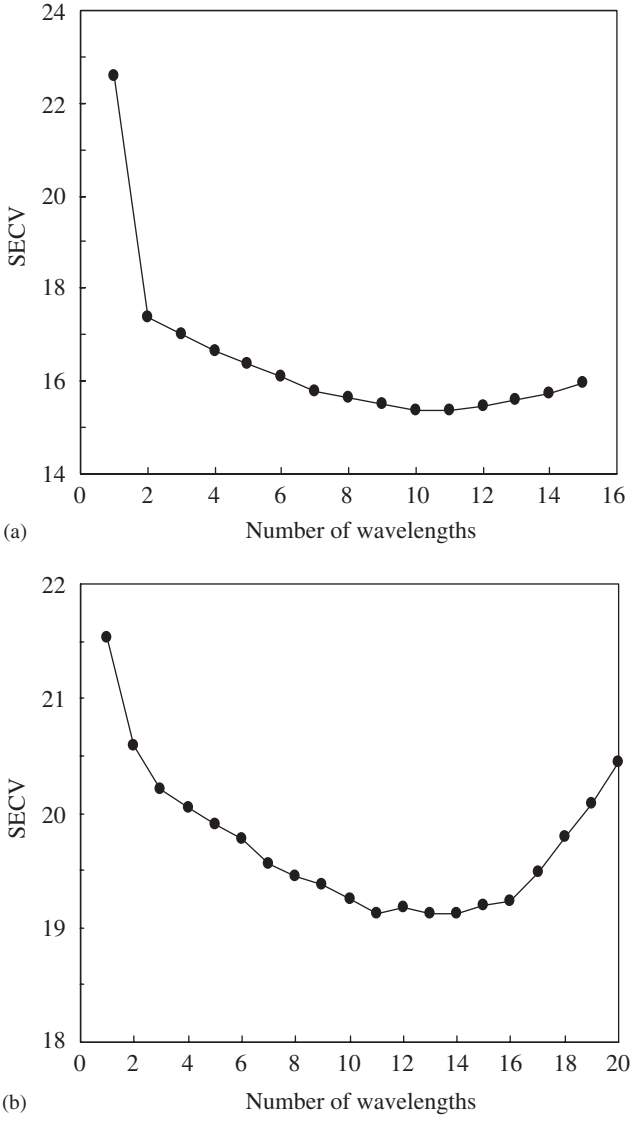

Fig. 7. Root mean squares error of cross-validation (SECV) for estimating fruit firmness versus the number of wavelengths used for 'Red Haven' (a) and 'Coral Star' (b) peaches when Lorentzian function parameters a and b were treated as independent variables; The minimal SECV was obtained when ten wavelengths were used for 'Red Haven' and 11 wavelengths for 'Coral Star'

with the four parameter combinations (*i.e.* a, b, $a \times b$, and a & b) for 'Red Haven' peaches. Among the four combinations, parameter b had the lowest coefficient of determination (r^2) of 0·67. The parameter combination a & b gave best firmness predictions with values for r^2 of 0·77 and the standard error of validation or SEV of 14·2 N. The results from a and $a \times b$ were close with values for r^2 of 0·72 and 0·73, respectively.

The overall firmness prediction results for 'Red Haven' peaches (*Fig. 8*) are better than those for 'Coral

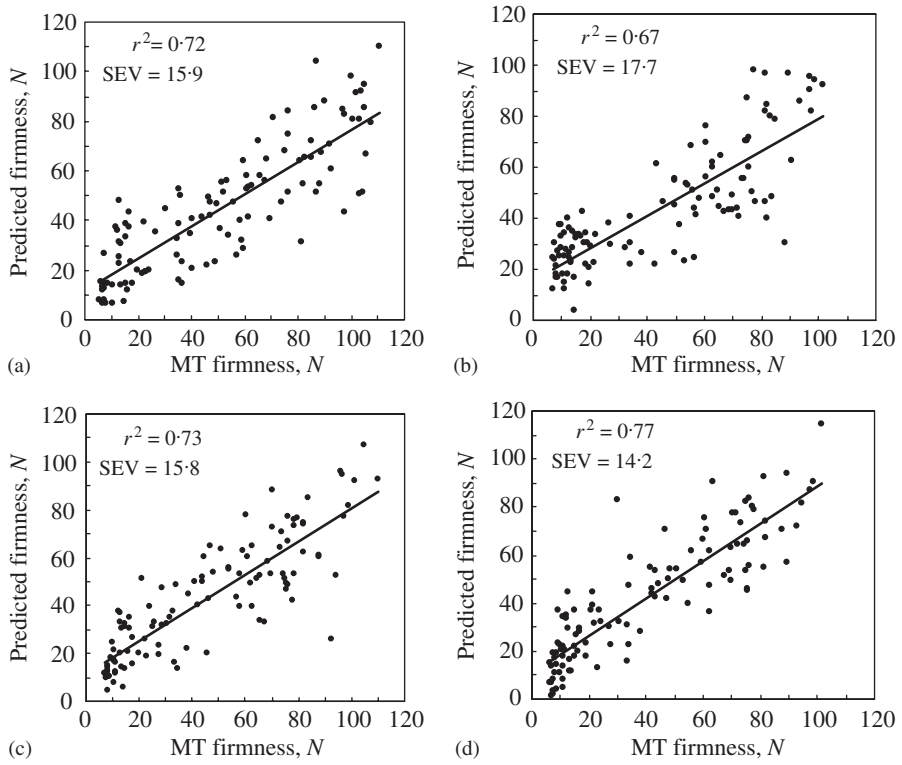

Fig. 8. Magness–Taylor (MT) firmness prediction results for 'Red Haven' peaches obtained with the four Lorentzian parameter combinations: (a) a, peak scattering value; (b) b, the full scattering width at one half of the peak value; (c) multiplication of a and b, or a × b; (d) two independent parameters a & b; r^2, coefficient of determination; SEV, standard error of validation

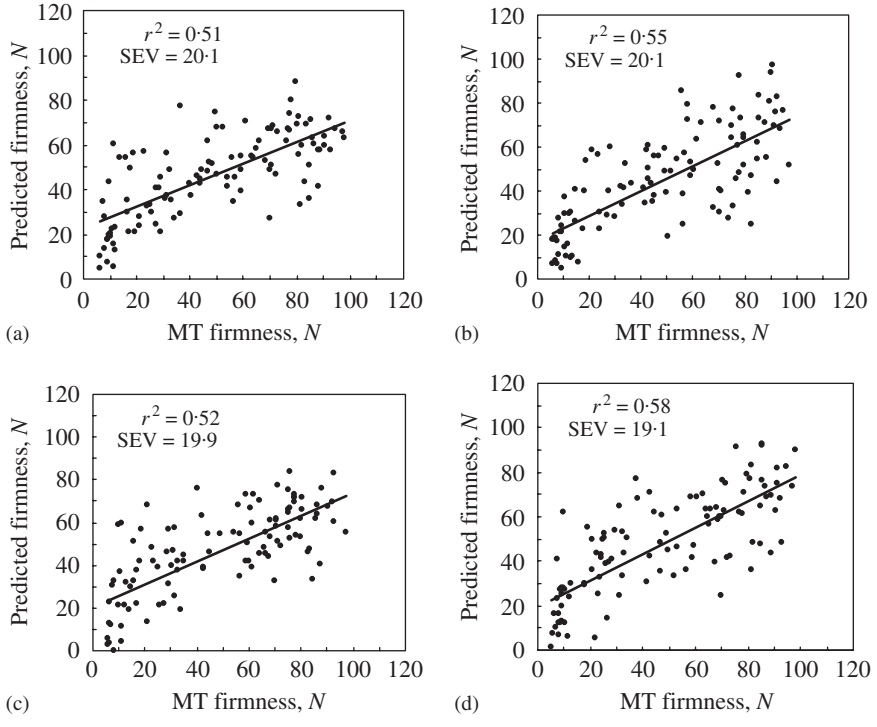

Fig. 9. Magness–Taylor (MT) firmness prediction results for 'Coral Star' peaches obtained with the four Lorentzian parameter combinations: (a) a, peak scattering value; (b) b, the full scattering width at one half of the peak value; (c) multiplication of a and b, or a × b; (d) two independent parameters a & b; r^2, coefficient of determination; SEV, standard error of validation

Star' peaches (*Fig. 9*). The best value for r^2 for 'Coral Star' was only 0·58 when the combination a & b was used. The other three parameter combinations yielded similar predictions with values for r^2 between 0·51 and 0·55.

Our firmness prediction results for 'Red Haven' peaches with the parameter combination a & b are comparable to the best results reported in literature by using the impact or sonic test (Hung *et al.*, 2001). Although the results for 'Coral Star' are relatively poor, they are also well within the middle range of the reported results with either the impact or sonic technique. Cultivar difference could be a factor affecting the relatively poor predictions for 'Coral Star' peaches. 'Coral Star' peaches had a higher percentage of soft fruit. The MT tester does not work as well with soft fruit as with firmer fruit, which could in turn affect the correlation for 'Coral Star' peaches. Furthermore, the MT firmness measurements are also known for lacking good repeatability due to both the inherent firmness variability within each fruit and the instrumental factor. This could be a limiting factor in obtaining high correlation for the current scattering method.

4. Conclusions

The Lorentzian function with two parameters a and b, where a is the peak scattering value and b is the full scattering width at one half of the peak value, accurately fitted the scattering profiles for peaches over the wavelength range between 600 and 1000 nm. Wavebands around 677 nm were most useful for predicting fruit firmness of both 'Red Haven' and 'Coral Star' peaches, reflecting the dominant effect of chlorophyll absorption on peach firmness. For 'Coral Star', the wavelengths around the 950 nm water absorption band were also found to be useful for firmness predictions. Ten or 11 wavelengths were needed to achieve the best predictions of fruit firmness. Among the four combinations of the two Lorentzian parameters ($a, b, a \times b$, and a & b), the combination a & b (in which a and b were treated as two independent variables) yielded best predictions of fruit firmness with values for the coefficient of determination r^2 of 0·77 and 0·58 for 'Red Haven' and 'Coral Star', respectively. Hyperspectral scattering is potentially useful for assessing peach fruit firmness.

Acknowledgements

The authors thank Mr. Benjamin Bailey, Engineering Technician, and Mr. Yonggang (Gary) Qin, Computer Programmer, for their technical support for this research. The research was supported in part by the USDA National Research Initiative Competitive Grant Program (USDA/NRI/CGP) under Grant #2002-35503-12285.

References

Abbott J A; Lu R; Upchurch B L; Stroshine R L (1997). Technologies for nondestructive quality evaluation of fruits and vegetables. Horticultural Reviews, **20**(1), 1–120

Cho Y J; Han Y J (1999). Nondestructive characterization of apple firmness by quantification of laser scatter. Journal Texture Studies, **30**(6), 625–638

Cubeddu R; D'Andrea C; Pifferi A; Taroni P; Torricelli A; Valentini G; Dover C; Johnson D; Ruiz-Altisent M; Valero C (2001). Nondestructive quantification of chemical and physical properties of fruits by time-resolved reflectance spectroscopy in the wavelength range 650–1000 nm. Applied Optics, **40**(4), 538–543

Dull G G; Birth G S; Smittle D A; Leffler R G (1989). Near infrared analysis of soluble solids in intact cantaloupe. Journal of Food Science, **54**(2), 393–395

Hung Y-C; Prussia S; Ezeike G O I (2001). Firmness-measurement methods. In: Nondestructive Food Evaluation—Techniques to Analyze Properties and Quality (Gunasekaran G, ed). Marcel Dekker, Inc., New York

Kawano S; Watanabe H; Iwamoto M (1992). Determination of sugar content in intact peaches by near infrared spectroscopy with fiber optics in interactance mode. Journal of Japanese Horticultural Sciences, **61**(2), 445–451

Lammertyn J; Nicolai B; Ooms K; De Smedt V; De Baerdemaeker J (1998). Non-destructive measurement of acidity, soluble solids, and firmness of Jonagold apples using NIR-spectroscopy. Transactions of the ASAE, **41**(4), 1089–1094

Lawrence K C; Windham W R; Park B; Buhr R J (2003). Hyperspectral imaging system for identification of fecal and ingesta contamination on poultry carcasses. Journal of Near Infrared Spectroscopy, **11**(4), 269–281

Lu R (2001). Predicting firmness and sugar content of sweet cherries using near-infrared diffuse reflectance spectroscopy. Transactions of the ASAE, **44**(5), 1265–1271

Lu R (2003). Detection of bruises on apples using near-infrared hyperspectral imaging. Transactions of the ASAE, **46**(2), 523–530

Lu R (2004). Multispectral imaging for predicting firmness and soluble solids content of apple fruit. Postharvest Biology and Technology, **31**(2), 147–157

Lu R; Abbott J A (2004). Chapter 5: force/deformation techniques for measuring texture. In: Texture in Food, Volume 2: Solid Foods (Kilcast D, ed). Woodhead Publishing Limited, England

Lu R; Ariana D (2002). A near-infrared sensing technique for measuring internal quality of apple fruit. Applied Engineering in Agriculture, **18**(5), 585–590

Lu R; Chen Y R (1998). Hyperspectral imaging for safety inspection of foods and agricultural products. In: Pathogen Detection and Remediation for Safe Eating (Chen Y R ed), Proceedings of SPIE—The International Society for Optical Engineering, **3544**, 121–133.

Lu R; Guyer D E; Beaudry R M (2000). Determination of firmness and sugar content of apples using near-infrared

diffuse reflectance. Journal of Texture Studies, **31**(6), 615–630

Martinsen P; Schaare P (1998). Measuring soluble solids distribution in kiwifruit using near-infrared imaging spectroscopy. Postharvest Biology and Technology, **14**(3), 271–281

McGlone V A; Abe H; Kawano S (1997). Kiwifruit firmness by near infrared light scattering. Journal of Near Infrared Spectroscopy, **5**(1), 83–89

McGlone V A; Kawano S (1998). Firmness, dry-matter and soluble-solids assessment of postharvest kiwifruit by NIR spectroscopy. Postharvest Biology and Technology, **13**(2), 131–141

Moons E; Dardenne P; Dubois A; Sindic M (1997). Non-destructive visible and NIR spectroscopy measurement for the determination of apple internal quality. Acta Horticulture, **517,** 441–448

Peng Y; Lu R (2004). A liquid crystal tunable filter based multispectral imaging system for prediction of apple fruit firmness. Proceedings of SPIE—The International Society for Optical Engineering, **5587,** 91–100

Peng Y; Lu R (2005). Modeling multispectral scattering profiles for prediction of apple fruit firmness. Transactions of the ASAE, **48**(1), 235–242

Peirs A; Scheerlinck N; De Baerdemaeker J; Nicolai B M (2003). Starch index determination of apple fruit by means of a hyperspectral near infrared reflectance imaging system. Journal of Near Infrared Spectroscopy, **11**(5), 379–389

Shmulevich I; Galili N; Howarth M S (2003). Nondestructive dynamic testing of apples for firmness evaluation. Postharvest Biology and Technology, **29**(3), 287–299

Slaughter D C (1995). Nondestructive determination of internal quality in peaches and nectarines. Transactions of the ASAE, **38**(2), 617–623

Tu K; De Busscher R; De Baerdemaeker J; Schrevens E (1995). Using laser beam as light source to study tomato and apple quality non-destructively. In: Proceedings of the Food Processing Automation IV Conference, 3–5 November 1995, Chicago, IL, pp. 528–536

Tuchin V (2000). Tissue Optics—Light Scattering Methods and Instruments for Medical diagnosis. SPIE Press, Washington, USA

Valero C; Ruiz-Altisent M; Cubeddu R; Pifferi A; Taroni P; Torricelli A; Valentini G; Johnson D; Dover C (2004). Selection models for the internal quality of fruit, based on time domain laser reflectance spectroscopy. Biosystems Engineering, **88**(3), 313–323